D13.3 OPTIDRILL drilling advisory system performance monitoring and evaluation (2nd Field Test Campaign)

Deliverable No	D13.3
Work package No. and Title	WP13 OPTIDRILL system field-scale test and validation in a borehole
Version - Status	V1.2 - Final
Date of Issue	17/12/2024
Dissemination Level	PUBLIC
Filename	D13.3 – v1.2

This project has received funding from the European Union's Horizon 2020 research and innovation action under grant agreement No 101006964

DOCUMENT INFO

Authors

Author	Organization	e-mail
Henning Knauer	IEG	henning.knauer@ieg.fraunhofer.de
Kevin Mallin	GEO	kevinmallin@geolorn.co.uk
Pufinji Obene	Oliveris	pufinjiobene@oliveris.com
Shahin Jamali	IEG	shahin.jamal@ieg.fraunhofer.de

Document History

Date	Version	Editor	Change	Status
16.12.2024	0.0	Henning Knauer, Kevin Mallin	Section 1, 2	Draft
16.12.2024	0.0	Henning Knauer	Section 3.1, 3.2	Draft
17.12.2024	0.4	Pufinji Obene	Section 3.3	Draft
18.12.2024	0.5	Shahin Jamali	Executive summary update	Draft
18.12.2024	1.0	Shahin Jamali	Editorial review	Final
29.04.2024	1.1	Kevin Mallin	KPI section	Draft
18.12.2024	1.2	Shahin Jamali	Editorial review	Final

TABLE OF CONTENTS

LIST OF FIGURES

LIST OF TABLES

EXECUTIVE SUMMARY

This deliverable reports on the second independent field test of the OptiDrill drilling advisory system and the sensor system at the Fraunhofer IEG site in Bochum, Germany. Initially planned as drilling simulations, the team opted for field-scale testing to better replicate real-world conditions, yielding more credible validation results.

During the test, the OptiDrill system monitored drilling parameters, including weight on bit (WOB) and rotational speed, over a depth of approximately 102 meters. The ROP prediction module achieved a Mean Absolute Error (MAE) of 1.89 m/h, identifying opportunities to enhance drilling efficiency by up to 19%. The lithology prediction module improved in accuracy compared to the first field test, but struggled with transitional formations, indicating a need for site-specific model retraining. The anomaly detection module flagged about 20% of data as anomalous, demonstrating its potential to identify operational risks. The sensor system effectively captured dynamic drilling parameters but faced limitations due to surface-level placement, which affected accuracy. Additional tests within the UK deployed the sensors directly in the drill string for improved validation. Furthermore, the KPIs that were defined at an earlier stage of the project within deliverable 1.5 are discussed and an outlook on the future steps is given. Overall, the field testing provided valuable insights into the OptiDrill system's capabilities, confirming its potential to optimize drilling performance and energy efficiency.

1. INTRODUCTION

Work package number 13 deals with the field testing of the OptiDrill system and the evaluation of the system's outputs generated by the integrated machine learning models. This report summarizes and evaluates the findings and outputs of the OptiDrill system from the second field test that was performed in at the IEG in Bochum, Germany. The OptiDrill system was tested in a similar manner as it had been during the first field test. Based on the findings from the first field test, which were stated in the previous report, the supervised learning-based machine learning model were retrained on the newly acquired data from the P1 wellbore.

In the first section of this report the changes to the OptiDrill software, especially the ROP prediction and the drilled lithology prediction models are described. A brief summary of the second field test is given and the results from the model retraining are presented and summarized.

In the second section of the report the results from the field test are evaluated. The dataset generated and processed during the drilling operation is analyzed and compared to the data the machine learning models were trained on. Afterwards the outputs of the three machine learning based software module for the ROP prediction and optimization, the drilled lithology prediction, and the drilling problem detection are evaluated following the same procedures as it has been reported on in the previous deliverable for the first field test. Insights into the testing of the OptiDrill sensor system are also given in the second section of the report. Within the third section of the report the KPIs that were defined in the public deliverable 1.5 at an earlier stage of the project are discussed.

Finally, a conclusion summarizing the findings from the second field test is given discussing the results, new insights, and shortcomings of the OptiDrill system and its application in a real drilling environment.

2. SECOND FIELD TEST IN BOCHUM

The second round of drilling within the Push-It project was conducted in early November, as described in the deliverable report D13.1. Again, just as during the drilling operation for the P1 wellbore the IEG joined the whole process for conducted a second field test of the OptiDrill software system. During the second field test the software was run for around 41 hours and a drilled depth of 102 meters was recorded and analysed using the OptiDrill system. The project partner Oliveris (formerly PVI) joined the drilling operation again and recorded data from around 80 metres until the end of the wellbore.

2.1 Field Test OptiDrill Software Settings and Model Retraining

The OptiDrill Drilling Advisory System was run in the same manner as it was reported on in the previous report. No major changes to the software system were applied after the first round of drilling. However, as it was decided based on the findings from the previous report the supervised-learning based machine learning models for the ROP prediction and the drilled lithology prediction were retrained based on the data from the P1 wellbore. Apart from the retraining of the models for the ROP optimization framework it was decided to remove the mud flow from the set of controllable parameters. This was done based on a discussion with the driller, since the mud flow was already at its maximum due to hardware limitations and should not be changed, especially lowered to guarantee proper flushing and cuttings transport to the surface.

2.1.1 ROP Prediction Model Retraining

The ROP prediction model that is the basis for the MSE based ROP optimization was retrained on the data from the first wellbore to try and improve the good results that could already be achieved during the first round of drilling a little further. For this purpose, a cross validation was performed and the transformer model for the ROP prediction was retrained on four folds of equal length of the P1 wellbore.

Table 1: ROP prediction k-fold-cross-validation results for retraining on the P1 wellbore

Fold	MAE [m/h]	RMSE [m/h]	R^2
0	0.91	1.31	0.96
1	0.89	1.34	0.94
2	0.94	1.34	0.97
3	0.86	1.12	0.80
Mean	0.9	1.28	0.92

The table above shows the results of the cross-validation of the transformer model on the P1 wellbore. Each of the sections of the four individual folds cover around 32 metres of consecutive drilled depth. Looking at the results from the cross validation it can be seen that performance metrics are all very good with an average MAE of 0.9 m/h, an average RMSE of 1.28 m/h, and an average R^2-Score of 0.92. The figure on the next pages gives an overview of the validation results of the 4 folds with the actual and the predicted ROPs plotted over the measured depth of the well.

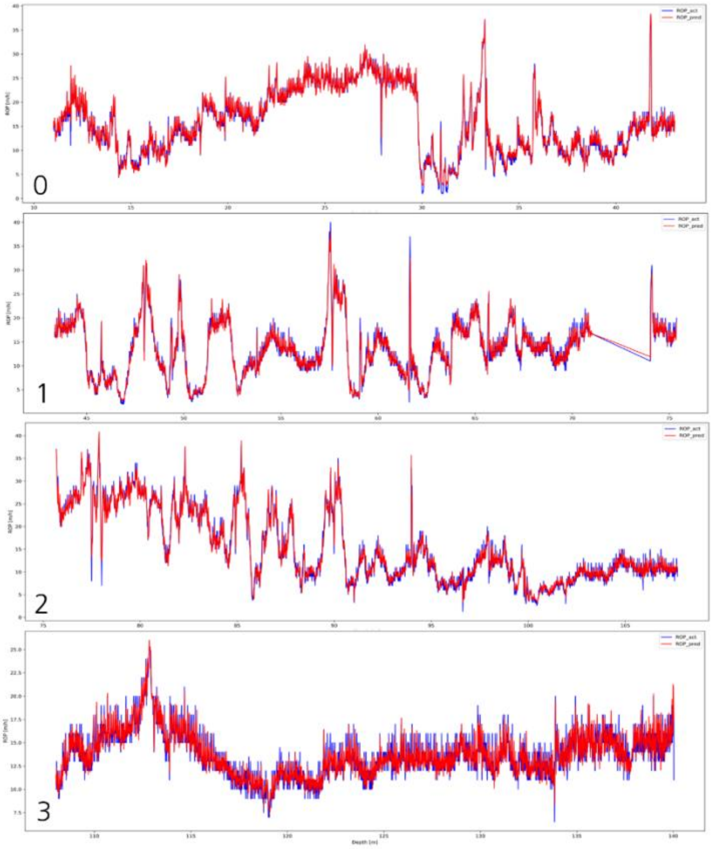

Figure 2: Actual ROP values in blue and predicted ROP values in red plotted over the measured depth of the P1 wellbore for all four folds of the cross validation

The table and the plots in the figure above show that the model's predictive performance is very consistent over all sections of the well. Based on the findings from the k-fold-cross-validation a ROP prediction model was trained on the whole wellbore dataset, while being validated on the last 20 metres, that was then later used for the second field test. The figure below shows the training process of the model with the training loss in blue and the validation loss in orange. The training was terminated by the implemented callbacks to prevent overfitting.

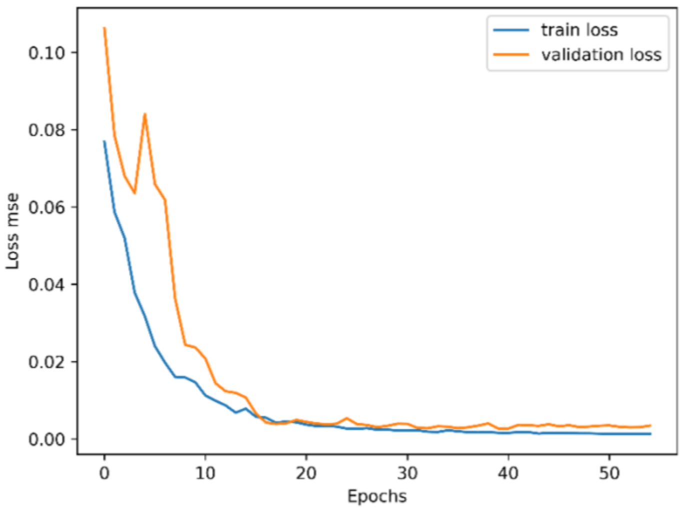

Figure 1: Train and validation losses of the ROP prediction model

2.1.2 Drilled Lithology Prediction Model Retraining

The 1D CNN drilled lithology prediction model was also retrained on the P1 wellbore dataset. However, since in this case we are dealing with a classification model, not with a regression model as in the previous section, it was not possible to perform a k-fold-cross-validation on consecutive section of the wellbore dataset. Since the lithology profile is not very diverse this would result in folds in which not all classes can be represented either in the data used for training or the data used for the validation of the model. Due to this limitation, it was decided to retrain and validate the drilled lithology model on a stratified random train-validation split. Stratified mean in this context that the balance between the classes in both splits will be guaranteed. The results of the training and validation of the 1D CNN model are shown in the following figures.

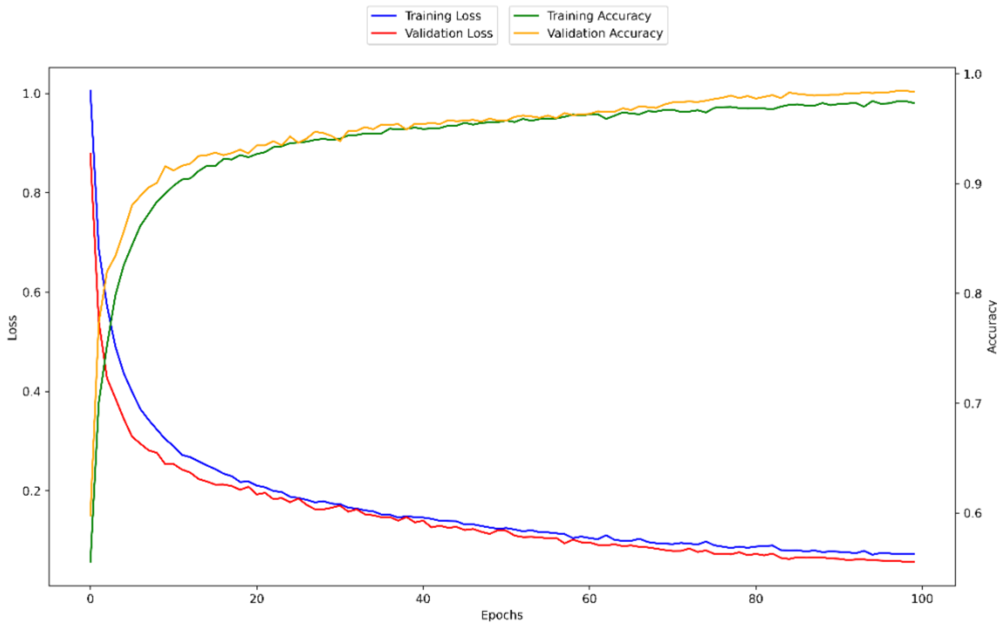

Figure 3: Train and validation loss and accuracy of the 1D CNN model trained on the P1 wellbore dataset

The train and validation losses and accuracies of the retrained drilled lithology prediction model shown in the figure above are very good with a final validation accuracy of 97%. However, the training approach used here due to the lack of diversity in the lithology profile and the lack of additional wellbore datasets, is not ideal as it has been discussed and justified in the deliverable reports from work packages 7 and 8. The results achieved during model training and validation are not expected to be reproducible during the field test, however since this time the model will be trained on the same set of classes that will be encountered, we expect better results than in the first field test and additional valuable insights from the evaluation of the model outputs.

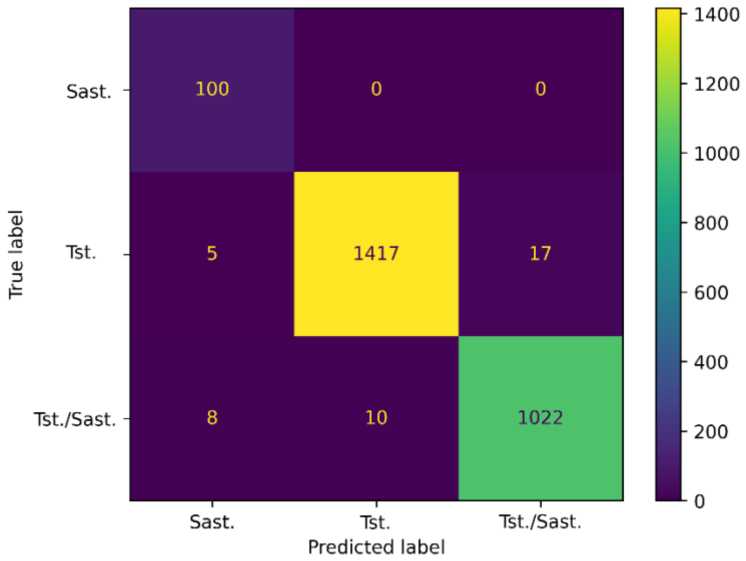

Figure 4: Confusion matrix of the retrained drilled lithology prediction model

The confusion matrix above shows the results of the validation of the lithology prediction model. During the validation barely any significant confusion with other classes occurred. The greatest, but still insignificant confusions occurred between the classes *Claystone* (Tst.) and *Claystone/Sandstone* (Tst./Sast.). In no instance was the class *Sandstone* (Sast.) confused with any of the other two classes. However, in some instances the other classes were incorrectly predicted as *Sandstone*.

Table 2: Individual performance metrics for the different lithology classes from the validation of the drilled lithology prediction model

	Sandstone	**Claystone**	**Claystone/Sandstone**
Precision	0.88	0.99	0.98
Recall	1.00	0.98	0.98
F1-Score	0.94	0.99	0.98
Support	100	1439	1040

The table above displays the performance metrics for the three lithology classes. All metrics show the same picture with very good results and only very few errors that occurred during the model validation.

3. FIELD TEST RESULTS AND EVALUATION

In this section we are reporting on the results and findings from the second round of field testing in Bochum. First, we are going to take a look at the data that has been gathered and processed by the OptiDrill system during the drilling operation. We will compare the dataset created during the second field test with the data from the first field test, which was used for training the ROP and drilled lithology prediction models. Afterwards we will look at the outputs of the three machine learning models.

3.1 Data Comparison

The following figure shows the plots of the drilling process parameters processed by the OptiDrill software system and used as input data for the machine learning models. The plots do not show any larger gaps in the data or other problematic areas. What can be observed in the plots is the change of the bottom hole assembly at around 29 metres depth. From that point on a clear change in the measured values for some of the drilling process parameters can be observed, e.g. for the torque and WOB which were very constant before and increased afterwards, or the mud flow which was also increased.

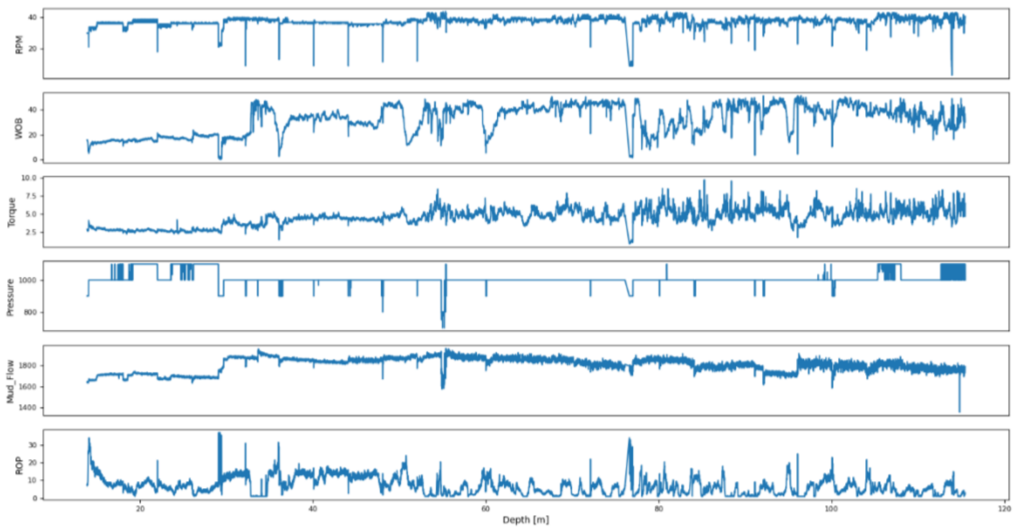

Figure 5: Plots of the drilling process parameters from the P2 wellbore processed and saved by the OptiDrill System

However, comparing the plots from the second wellbore to those of the first wellbore some significant differences can be observed, which are even more obvious when comparing the statistical overviews of both datasets. The following two tables show the statistical overviews of the P2 and the P1 wellbore datasets that have been processed by the OptiDrill system. Since the P1 wellbore was drilled deeper than the P2 wellbore, for the statistical overview of the P1 dataset only the same depth range was used as in the P2 dataset.

Table 3: Statistical overview of the P2 wellbore dataset from the second field test

	Depth_m	RPM_rpm	WOB_kN	TRQ_kNm	P_P_kPa	MFI_lpmin	ROP_mph
mean	64.63	37.50	32.31	4.47	1009.01	1803.70	6.91
std	29.41	3.10	11.29	1.12	39.52	66.35	4.84
min	13.90	3.00	0.10	0.88	700.00	1358.50	1.00
25%	39.16	36.00	21.48	3.80	1000.00	1758.00	3.00
50%	64.48	37.50	34.92	4.54	1000.00	1820.42	6.20
75%	90.27	39.00	42.21	5.20	1000.00	1856.00	9.75
max	115.43	44.00	51.11	9.66	1100.00	1958.00	37.00

Table 4: Statistical overview of the P1 wellbore dataset from the first field test

	Depth_m	RPM_rpm	WOB_kN	TRQ_kNm	P_P_bar	MFI_lpmin	ROP_mph
mean	64.74	36.28	47.21	4.86	1092.46	1676.04	15.27
std	29.71	3.51	17.71	0.76	28.43	37.67	6.85
min	13.90	7.00	0.00	1.18	1000.00	1548.00	1.00
25%	39.20	35.00	30.71	4.32	1100.00	1647.33	10.00
50%	63.59	36.00	49.44	4.92	1100.00	1680.00	14.00
75%	91.04	38.67	60.43	5.37	1100.00	1703.00	19.50
max	115.43	44.00	105.07	7.90	1200.00	1760.50	40.00

Comparing the two tables, especially for the drilling process parameters WOB and the ROP significant differences can be seen in the statistical overview. The WOB values of the second round of drilling are significantly lower, the mean WOB of the P2 wellbore is at 32 kN, while the mean value of the P1 wellbore lies at around 47 kN. This can be explained due to the limitation of the WOB values that has been applied because of the new, much heavier BHA that was used for the P2 wellbore. Comparing the ROP values of the two values it is obvious that the P2 wellbore was drilled much slower. The mean ROP of the P2 wellbore lies at 6.9 m/h while the mean ROP of the P1 wellbore is more than twice as high with almost 15.3 m/h. This is also caused by the limitations in WOB and ROP that have been decided on to reduce the risk of deviations from the vertical in the wellbore path. Apart from these two parameters the mud flow was also increased in the second wellbore, but not as significantly as the other two parameters WOB and ROP.

3.2 Machine Learning Model Evaluation

In this section of the report the outputs of the machine learning based modules of the OptiDrill software will be evaluated in the same manner as they have been in the previous report. Since for the second round of field testing the ROP prediction and the drilled lithology prediction models have been optimized and retrained on the data from the first field test, we will compare the results achieved in both runs in each section.

3.2.1 ROP Prediction and Optimization Module

The following table shows an overview of the errors made by the ROP prediction model. The MAE lies at 1.89 m/h, the RMSE at 2.47 m/h, and the R^2-Score at 0.78. All three error metrics calculated are better than those that were achieved during the first field test. Looking at the sign of the errors made it can be seen that compared to the first round of drilling the model more optimistic predictions that were higher than the actual ROP value with a higher average positive error. This can be explained by the fact that the model was trained on a dataset with significantly higher ROP values than those that were achieved.

Table 5: ROP prediction mode error evaluation

ROP Errors	MAE [m/h]	1.89
	RMSE [m/h]	2.466586
	R2-Score	0.777345
	Instances with positive error	6348
	Average positive error [m/h]	2.24
	Instances with negative error	3420
	Average negative error [m/h]	-1.23

The difference in ROP values was described in the previous section and was caused by the limitation in ROP and WOB in order to prevent the drill path from deviating.

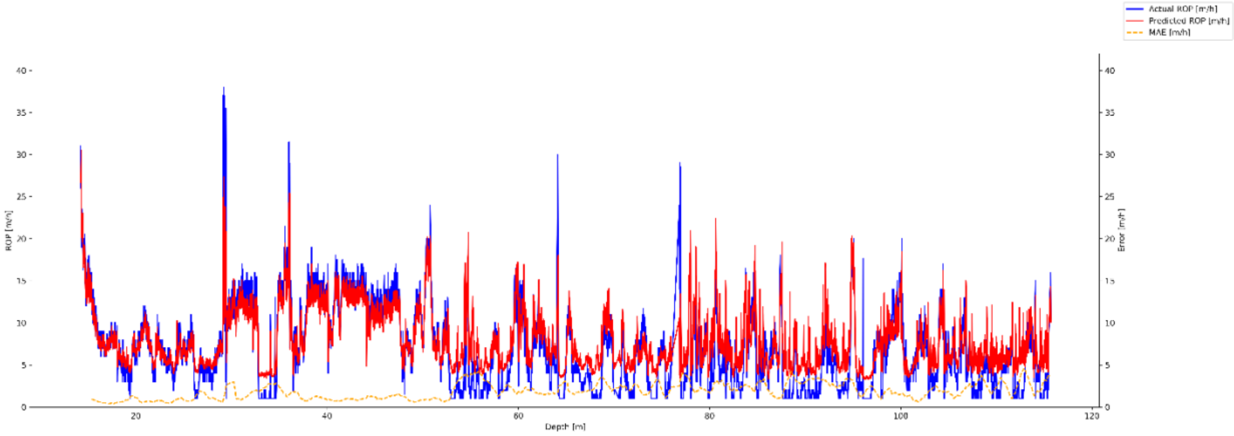

Figure 6: Actual ROP in blue and predicted ROP in red plotted over the measured depth. The MAE for a window of 100 data points is plotted in orange.

The plot above shows the actual ROP values recorded during the drilling operation alongside the values that were predicted by the model. Additionally, the MAE for a window of 100 consecutive predictions was plotted in orange. The trend of predicting higher ROP values can be clearly seen in the plots, especially in the last two thirds of the wellbore. It can also be seen that the prediction in the first section of the wellbore, until around 29 metres, are more on point that the rest. This is due to the fact that for the first section the same BHA was used as for the first wellbore. This can be very clearly seen in the following two figures comparing the predictions from the first section of the well with the old BHA with another section with the new BHA.

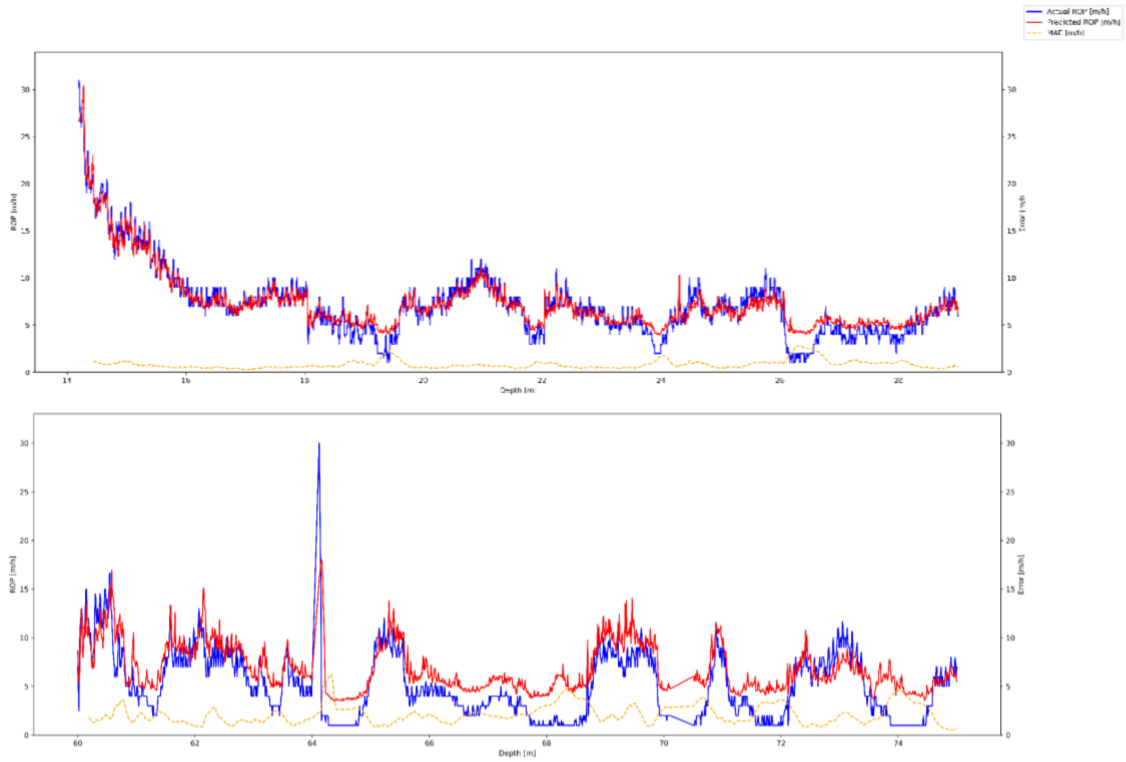

Figure 7: Comparison of the prediction of two sections with equal length and different BHAs

Table 6: Statistical overview over the different ROP values

	Actual ROP	Predicted ROP	Optimised ROP
Average ROP [m/h]	6.68	7.70	7.74
Standard deviation [m/h]	4.52	3.30	3.30
Min. ROP [m/h]	1.00	3.30	3.17
Max. ROP [m/h]	38.00	30.47	29.12
Percentile 50% [m/h]	6.00	6.76	6.81
Percentile 75% [m/h]	9.00	9.59	9.61
Percentile 90% [m/h]	13.00	12.57	12.63
Percentile 95% [m/h]	14.67	13.80	13.89
Percentile 99% [m/h]	18.00	17.53	17.79

The table above shows a statistical overview of the actual ROP values recorded during the drilling operation, the predicted ROP values based on the measured drilling process parameters, and the fictitious optimised ROP values based on the systems recommendations. Comparing the actual with the predicted ROP values the average predicted ROP values are about 1 m/h higher, while the standard deviation is around 1.2 m/h lower for the predictions. Also, it looks like the model is struggling to predict very low ROP values. The last column, showing the statistical properties of the optimised ROP values, shows that the average optimised ROP value is just insignificantly higher than that of the actual ROP. Looking at the percentiles it can be seen that this applied to every single percentile that was calculated.

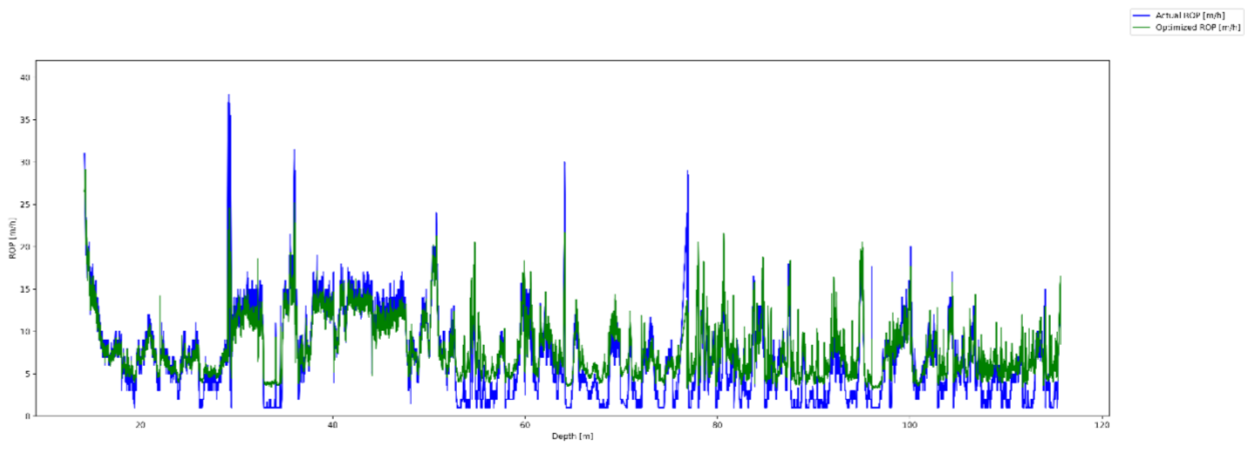

Figure 8: Actual ROP in blue and optimised (expected ROP) plotted in green over the measured depth

The figure above shows the actual ROP values in blue plotted over the measured depth alongside the optimised, expected ROP values in green. The plots show that the optimised ROP values are on average significantly higher than the actual ROP values, which is to be expected since the predicted ROP values showed the very same trend.

Table 7: Actual and optimised MSE values

	Actual MSE	Optimised MSE
Average MSE [N/mm2]	232.21	92.46
Standard deviation [N/mm2]	244.31	38.03
Min. MSE [N/mm2]	0.64	0.68
Max. MSE [N/mm2]	1406.08	176.98

Table 8: ROP and MSE optimisation overview

ROP Optimisation	
Average ROP enhancement [m/h]	1.06
Average ROP enhancement [%]	69.11
Increased ROP values	9782
Decreased ROP values	0
Constant ROP values	0

MSE Optimisation	
Average MSE enhancement [N/mm2]	139.75
Average MSE enhancement [%]	36.25
Decreased MSE values	9348
Increased MSE values	433
Constant MSE values	1

The tables above give an overview of the MSE and ROP values in context of the optimisation based on the controllable drilling process parameters. The first table compares the actual with the optimised MSE values. It shows that the average MSE values is significantly lower than the average actual MSE value. However, due to the model's strong tendency to predict ROP values higher than the actual ROP, these values cannot be trust to full extent.

The other two tables show an overview of the impact of the optimization on the theoretical ROP and MSE values that were predicted and calculated. The optimised ROP value was higher than the actual ROP value in all cases with an fictitious average ROP enhancement of around 1 m/h. Looking at the MSE optimisation the optimised MSE value was lower than the actual value in around 96% of the cases with an average MSE reduction of around 140 N/mm². Of course, due to the tendency of the ROP prediction model to predict optimistically with an average positive error of over 2 m/h, these values need to be interpreted in this given context.

Table 9: Recommendations for the controllable drilling process parameters by the OptiDrill system

	Process Parameter	
Recommended Action	**RPM**	**WOB**
Increase	0	9781
Decrease	9782	0
Constant	0	1

The table above gives an overview of the recommended action by the OptiDrill system to optimise the ROP based on the MSE. It can be seen that these actions were very one-sided during the second field test. The RPM was always recommended to be lowered, just as it was for the first field test, and the WOB was always recommended to be increased. This makes sense since the WOB was limited to a lower value during the second field test as mentioned before.

3.2.2 Drilled Lithology Prediction Module

The drilled lithology prediction model has been retrained on the data from the first round of drilling and tested during the second drilling operation. The following table shows an overview of the prediction of the model and the distribution of the actual classes.

Table 10: Drilled lithology prediction model outputs from the second field test in Bochum

Lithology	Predicted Classes	Sandstone	56
		Claystone/Sandstone	4272
		Claystone	5454
	Actual Classes	Sandstone	498
		Claystone/Sandstone	5037
		Claystone	4247
	Predictions	True	3414
		False	6368

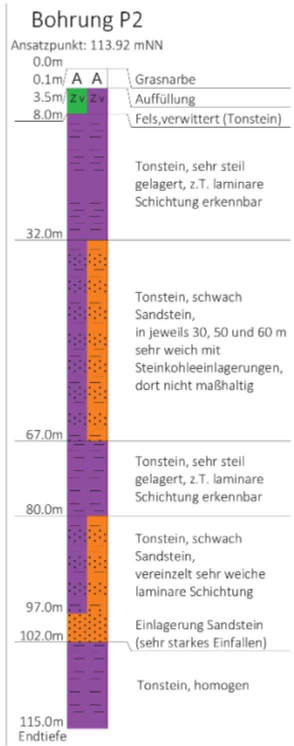

Figure 9: Preliminary lithology log Push-It P2 wellbore (created by Stefan Klein, CC Bergbaufolgenutzung, IEG)

The lithology prediction model was trained on the same classes that were determined during the logging of the second wellbore. It has to be noted that the lithology log that was used for the evaluation of lithology prediction model outputs on the second wellbore was a preliminary version, however due to time constraints this version had to used. The table shows that the distributions of the prediction lithology classes do look reasonable. All classes have been predicted, although the class sandstone, which is a minority class, has only been predicted in about 56 cases. All in all, the accuracy that could be achieved lies at around 35%, which is significantly lower that the accuracy that was achieved during the model retraining. This was expected and looking at the results it is very likely that the model overfitted to the training data, causing its ability to generalize and transfer its predictive capabilities to new data that is introduced to the model.

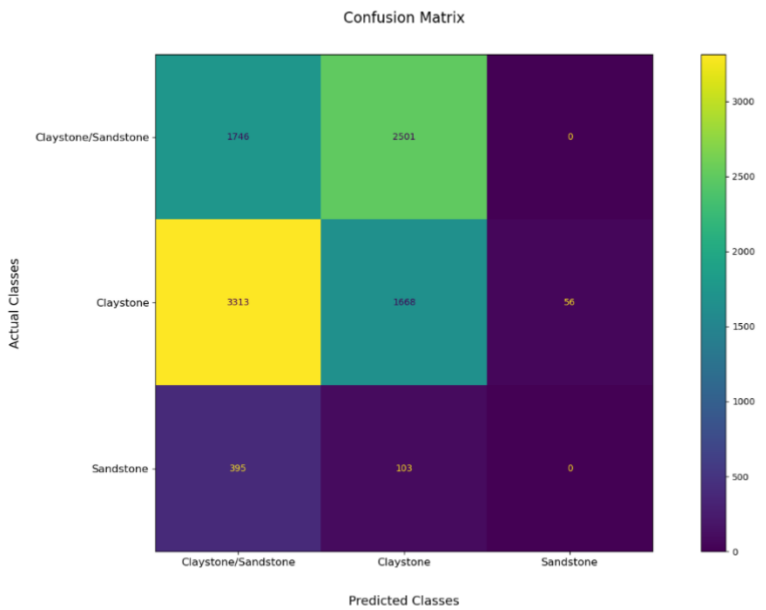

Figure 10: Confusion matrix of the model predictions for the Push-It P2 wellbore

Table 11: Individual performance metrics for the different lithology classes from the validation of the drilled lithology prediction model

	Claystone	Claystone/Sandstone	Sandstone
Precision	0.32	0.39	0.00
Recall	0.41	0.33	0.00
F1-Score	0.36	0.36	0.00
Support	4247	5037	498

The confusion matrix and the table above give further details about the drilled lithology prediction model's outputs during the second field test. Looking at the confusion matrix it can be seen that there are a lot of confusions between the classes *claystone* and *claystone/sandstone*. Apart from that it can be seen that no single instance of the class *sandstone* has been predicted correctly. The majority of the instance falsely classified as sandstone were misclassified as *claystone/sandstone*. The table with the respective performance metrics of the individual classes confirms these observations.

All in all, it can be concluded that the drilled lithology prediction model's performance did improve compared to its performance during the first field test. The predictions show more diversity and all lithology classes have been learned and output by the model. However, the quality of the predictions made is not satisfactory. Many confusions occur between the three classes, of which some are comprehensible, e.g. that many instances of the classes *claystone* and *claystone/sandstone* are confused or that the majority of the predictions of the class *sandstone* actually belong to the class *claystone/sandstone*. The most obvious reason for this is the lack of data. Although, the location of the Push-It wellbores is not too far from other locations for which a reasonable amount of data is available, such as the Geostar 2 which was used for training the model in the first run, the local lithologies still differ and require new data to enable a reliable classification. The second most likely reason is overfitting on the training data from the first wellbore. Since again, the statistical properties of the dataset that has been recorded during the second wellbore have changed significantly compared to those of the first wellbore, the model might be too adapted to the data from the first wellbore, leading to poor predictive performance.

3.2.3 Drilling Problem Detection Module

Since no optimizations have been implemented in the anomaly detection based drilling problem detection module, no significant differences should be expected. The following table shows an overview of the predictions made by the model during the second field test.

Table 12: Anomaly detection model outputs

Anomaly Detection	Predictions	9779
	Anomalous	2295
	Not anomalous	7484

Around 23% of the data points that have been analysed by the anomaly detection framework have been classified as anomalous. This falls in a comparable range than during the first field test of the OptiDrill system where around 20% of the data points were classified as anomalous. However, no actual drilling problem was encountered during the drilling operation.

3.3 Novel sensor system data and interpretations evaluation

3.3.1 Evaluation of Gain, Coherency, Angular Velocity (ω), and Specific Rock Energy (SRE) Analysis.

The analysis examines Gain (dB), Coherency, Angular Velocity (ω, in rad/s), and Specific Rock Energy (SRE) across transitional and non-transitional regions. Observations are derived from Sensor Subsystems 57 and 59, with references to packet numbers and corresponding figures.

At 12:15, during bunker reach, packet number 310 (Figure 11), packet number 315 (Figure 12), and packet number 330 (Figure 13) capture sensor responses. Figure 11 (packet 310) reflects the pre-transition state, where Gain and Coherency are stable, and SRE remains consistent, indicating minimal disturbance in the system. Angular Velocity (ω) at this stage is steady, suggesting rotational dynamics are not significantly impacting the observed signals. However, in Figure 12 (packet 315), Gain exhibits notable fluctuations, Coherency decreases, and SRE rises, pointing to increased energy demands as the system interacts with more resistant rock formations during the transition. These changes are accompanied by minor variability in ω, potentially amplifying signal disturbances. Figure 13 (packet 330) demonstrates post-transition stabilization, with Gain and Coherency normalizing as SRE decreases, indicating a return to more manageable energy conditions. Angular Velocity also steadies, reflecting improved operational stability.

At 13:20, packet number 620 (Figure 14), packet number 637 (Figure 15), and packet number 657 (Figure 16) highlight system behavior. Figure 14 (packet 620) shows pre-penetration conditions, where Gain and Coherency begin to vary slightly, and SRE starts to increase as rock resistance intensifies. Angular Velocity is stable, playing a secondary role in signal behavior. In Figure 15 (packet 637), representing the critical penetration phase, Gain shows significant variability, Coherency decreases sharply, and SRE peaks, reflecting the maximum energy demand needed to penetrate the formation. During this phase, any fluctuations in ω exacerbate instability by influencing how signals interact with the high SRE conditions. In Figure 16 (packet 657), post-penetration responses show stabilized Gain, improved Coherency, and reduced SRE as the system acclimates to the fully penetrated environment. Angular Velocity returns to a steady state, supporting uniform sensor performance.

The relationship between Angular Velocity, Gain, and SRE is most evident in transitional phases, such as those represented by packets 315 and 637. Variability in ω during these phases magnifies the effects of increased SRE, leading to pronounced fluctuations in Gain and reduced Coherency. This dynamic interplay highlights the challenges of maintaining signal integrity under high-energy-demand conditions. Conversely, in non-transitional areas such as packets 310, 330, 620, and 657, a steady ω correlates with stable SRE, consistent Gain, and higher Coherency, reflecting a more controlled and predictable environment.

In conclusion, Angular Velocity plays an amplifying role in transitional zones by intensifying the effects of rising SRE on Gain and Coherency. In non-transitional areas, steady ω and lower SRE contribute to system stability, underscoring the interconnected nature of these variables in both dynamic and steady-state operations. This analysis provides critical insights into the influence of SRE and rotational dynamics on sensor performance.

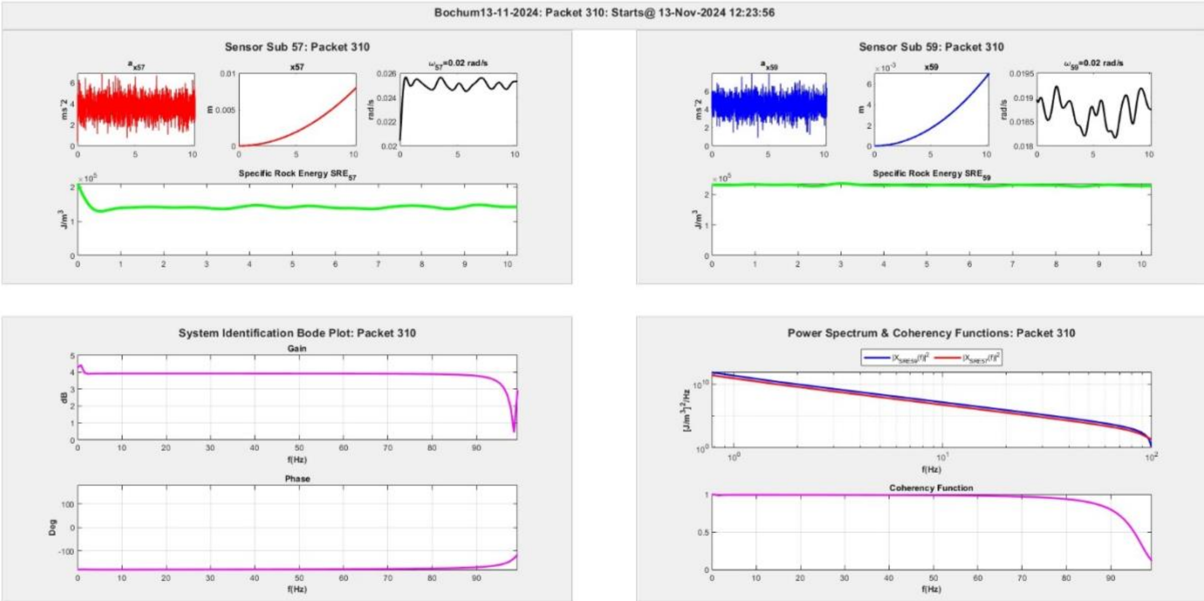

Figure 11: Packet number 310 for Sensor sub 57 and 59 along with their analysed Gain, Phase and Coherency function.

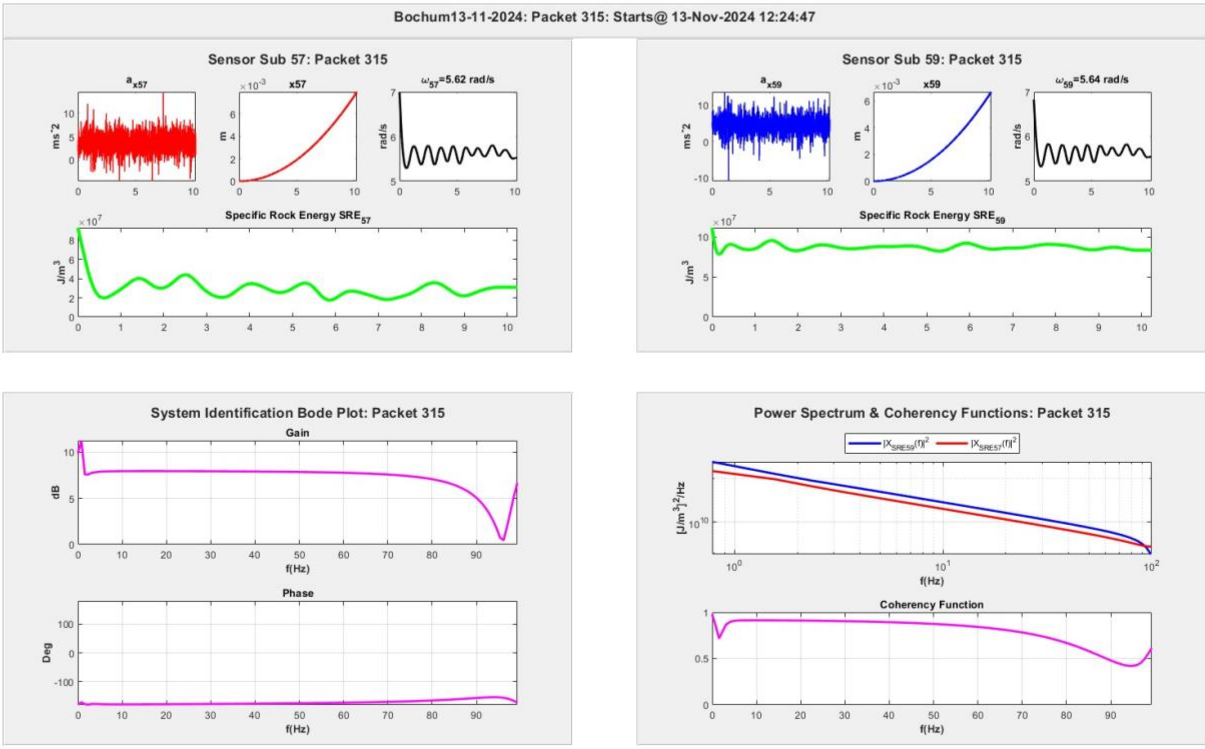

Figure 12: Packet number 315 for Sensor sub 57 and 59 along with their analysed Gain, Phase and Coherency function.

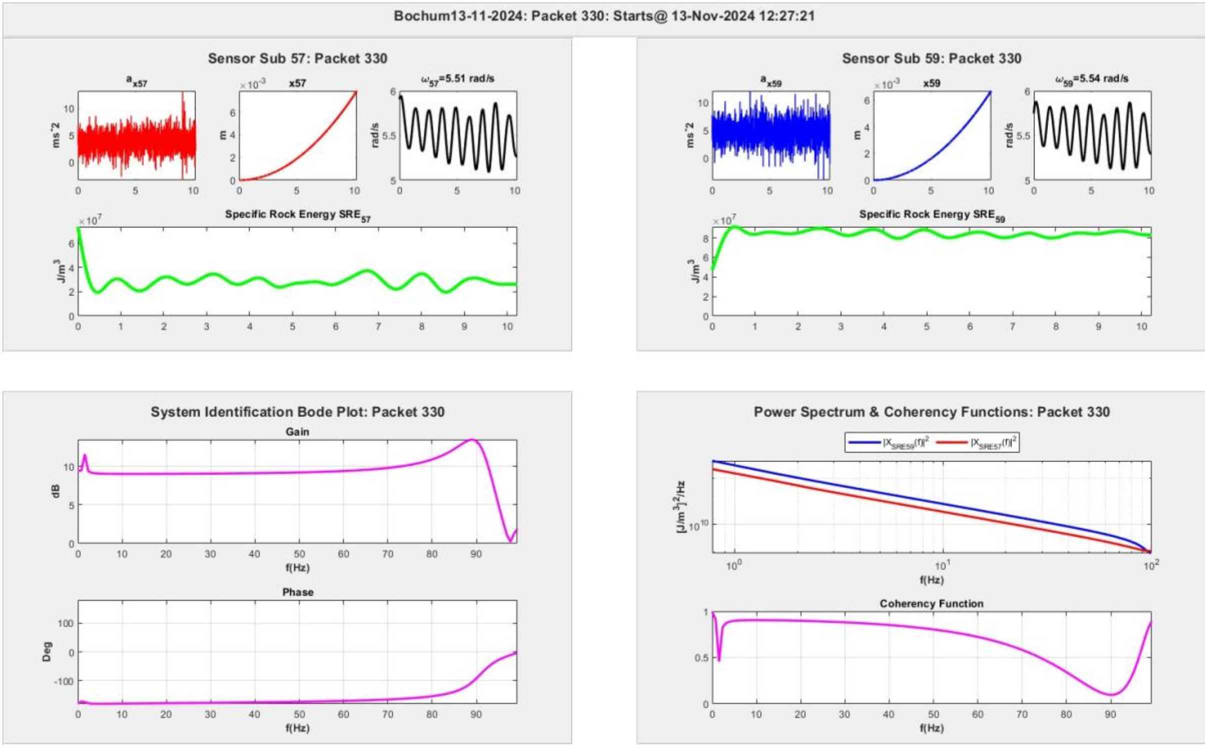

Figure 13: Packet number 330 for Sensor sub 57 and 59 along with their analysed Gain, Phase and Coherency function.

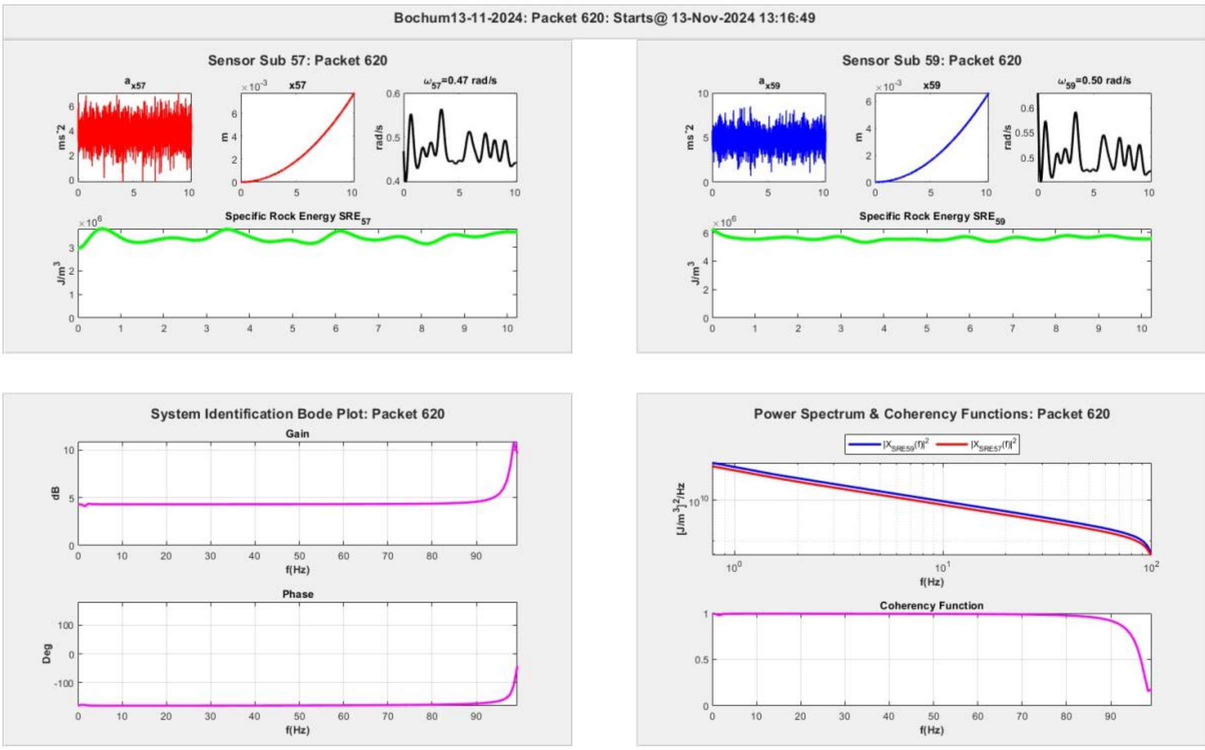

Figure 14: Packet number 620 for Sensor sub 57 and 59 along with their analysed Gain, Phase and Coherency function.

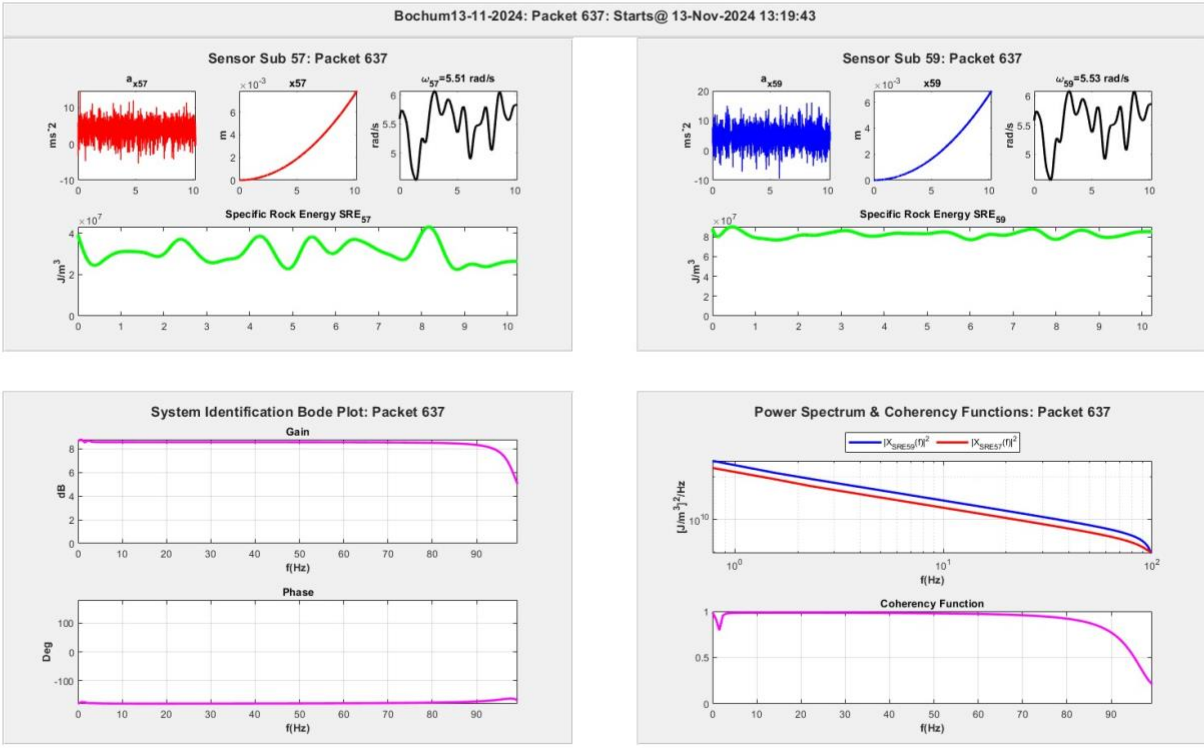

Figure 15: Packet number 637 for Sensor sub 57 and 59 along with their analysed Gain, Phase and Coherency function.

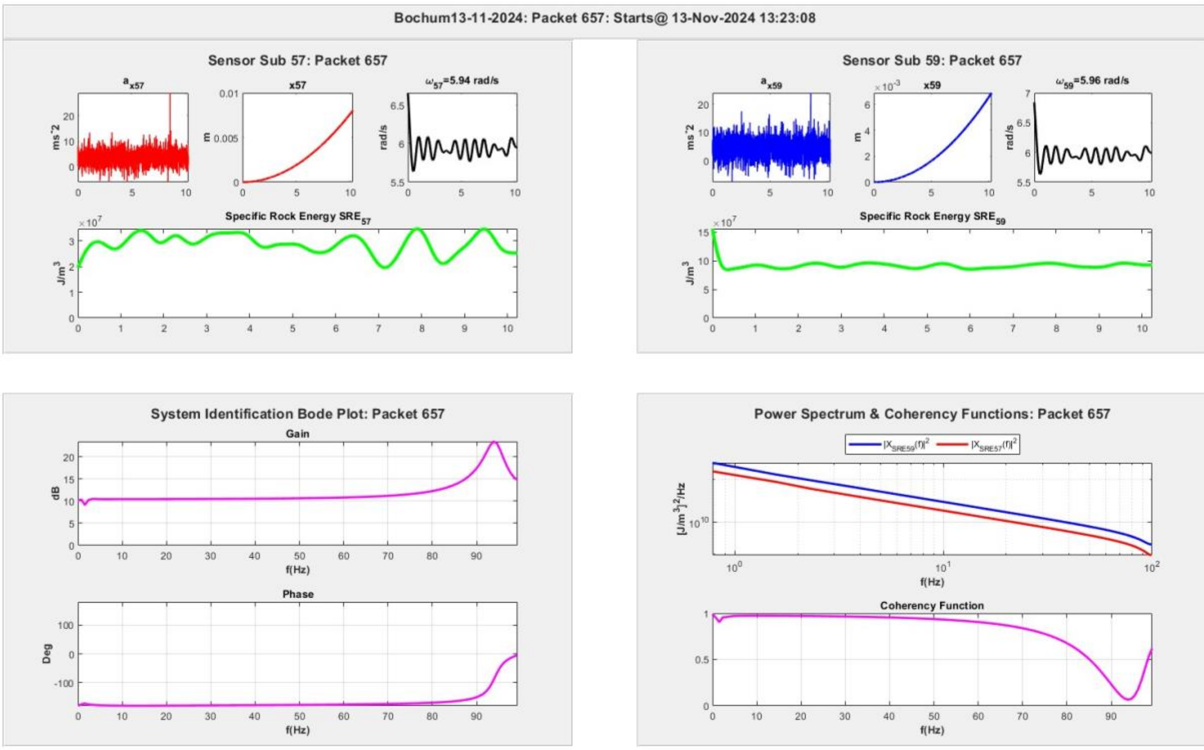

Figure 16: Packet number 657 for Sensor sub 57 and 59 along with their analysed Gain, Phase and Coherency function.

3.4 Summary of Differences in Measurement and Calculation

Force (F) measurements at the drill bit interface accurately represent tangential forces acting directly on the rock, whereas top tie-in sensors capture forces inflated by upstream mechanical losses. Similarly, rotational speed (ω) at the drill bit reflects true cutting dynamics, while upstream measurements are skewed by torsional oscillations and stick-slip effects. The rate of penetration (R), directly measurable at the bit, is often delayed or inaccurately inferred from top tie-in data. Consequently, SRE accuracy is higher at the drill bit interface but overestimated when derived from top tie-in data due to compounded mechanical losses.

4. KEY PERFORMANCE INDICATORS

At an earlier stage of the project within the public deliverable report D1.5 a list of key performance indicators (KPIs) was defined. The KPIs were assigned with a ranking ranging from “Bronze” over “Silver” to “Gold” describing possible fulfilment stages of the respective KPI. The KPIs focused on aspects of the project such as historic and training data, what-if-analysis, drill bit sensors and formation interaction, live data, and advisory system user interface. The following table gives an overview of the KPIs defined in D1.5.

Table 13: Key Performance Indicators from D1.5

KPI	Definition	Bronze	Silver	Gold
Historic & Training Data	Historic Drilling Data from Sedimentary Basin(s).	O&G wells, low temperature, but full suite of data. Varied drilling technologies deployed.	O&G Wells, plus hydrothermal geothermal brine wells. Possibly radiused and Extended horizontal section.	O&G Wells, plus hydrothermal geothermal brine wells. Possibly radiused and Extended horizontal section. Varied drilling technologies deployed. Well issues including overpressure (fluid/gas flows encountered) and well bore stability issues (breakout).
	Historic Drilling Data from wells in active volcanic settings.	Wells drilled with no issues, but complete suite of data.	Wells drilled with partial/complete losses, some steam kicks and quenching.	Wells drilled with “flash boiling”, partial to full loss of control, stuck/lost pipe.
	Historic Drilling Data from wells in igneous formations.	Wells drilled with no issues, but complete suite of data.	Wells drilled through fault zones, possible fluid Lost Circulation Zones. Both percussion and rotary drilling methods deployed.	Wells drilled completely with percussion. Wells drilled completely with rotary. Drilling issues encountered.
	Historic Drilling Data from wells in meta-sediments and igneous, contact/transition zones.	Wells drilled with no issues, but complete suite of data.	Wells drilled through fault zones, possible fluid Lost Circulation Zones. Both percussion and rotary drilling methods deployed.	Wells drilled completely with percussion. Wells drilled completely with rotary. Drilling issues encountered.
	Historic Drilling Data from wells in complex	Wells drilled with no issues, but complete suite of data.	Wells drilled through complex faulted and folded	Possible previous human activity – mining, depleted hydrocarbon wells.

	geological settings – pyroclastic flows, igneous intrusions in sedimentary basins, Basalt flows over sediments etc.		formations. Well stability issues.	Wells drilled through complex faulted and folded formations. Well stability issues. Well control issues. Possible previous human activity – mining, depleted hydrocarbon wells. SoA drilling methods.
What-If Analysis	What-If Analysis of historical well data	Poor data set(s) or data that has poor outcomes. What-If analysis provides full optimal outcome, fully validated in test wells (simulated/actual)	Partial data set(s), with enhanced analysis, in variable geological settings, fully validated in test wells (simulated/actual)	Full data set(s) available in complex geological setting(s) and training data fully validated in test wells (simulated/actual)
Drill Bit Sensors and Formation Interaction	New OptiDrill Sensors	Provide real-time data for most drilling methods	Provide real-time data for most drilling methods and operate with existing MWD systems	Provide real-time data for most drilling methods and operate with existing MWD systems across complex and harsh geological settings
Live Data	OptiDrill Sensors	Basic data transmitted in real-time	Lithological data, formation characteristics and basic drilling data transmitted in real-time	Complex drilling and predictive formation data transmitted in real-time
	OptiDrill Sensors & MWD/LWD systems	Basic data transmitted and recorded in real-time. Works in tandem for directional drilling programmes	Works with other advanced down hole sensor systems e.g. seismic while drilling, Electron Pulse etc., to provide enhanced well data in real-time	Able to work with complex drilling systems e.g. Rotary Steerable Systems and provide high quality real-time data.
Advisory System User Interface	Training Data/Real Data	ML System provides basic, previously lag-time, information in real-time	ML system provides information with a “menu” of options	ML system provides information and optimisation options in real-time
	Industry Adoption	20%	30%	>50%

Projects always define KPI's in the early stages of the work, often combined with Technology Roadmaps, this helps both the team working within the project, understand and gauge how their work is progressing and to external viewers, how the work may become applicable to their requirements. As projects develop towards maturity, a better method of looking at things is through Objectives and Key Results (OKR's). This allows both internal and external stakeholders to gauge results, measured against the project's objectives.

The objectives of the OptiDrill project were to develop a drilling advisory system that would benefit geothermal projects through ML/AI applications, using both historical and legacy data, as well as generating new data from field validation tests. Added to this were the developments of a user interface and downhole data sensors, that would operate within any BHA, and with any drilling system.

Table 1 shows how the KPI's were defined within the early stages and how they were ranked for the purposes of the project's progress. Whilst some were missed, most of the key objectives were achieved, as the results clearly demonstrate. In the field validation tests undertaken at Bochum, drilling data generated in real-time was clearly shown on the user-interface, which tied in with the training data and the data captured on USB memory sticks, positioned within the sensor subs, recorded the lithology accurately, when analysed.

These key results will now form the cornerstone for the next steps of product development within a commercial setting. Again, the objectives remain unchanged, but the key results will be matched to the original KPI's, wherein training data either from offset wells, or from newly drilled wells, informs the drilling team of the lithology, the ROP prediction and anomalous occurrences, and allows them to optimise the parameters that they can control. It has already been demonstrated that the OptiDrill system is agnostic to drilling methodology and can be set within the BHA, easily and the user-interface is both simple to use and set-up.

As the lithology prediction increases in accuracy and real-time data feeds into the 'downhole picture', it will enhance the completion programme of wells, through the avoidance of unnecessary drilling and for setting casings, screens etc., to enhance resource recovery, extend well life cycles and reduce associated risks going forwards.

5. CONCLUSION

The second round of drilling for the field testing and evaluation of the OptiDrill software system has yielded further important insights into the performance of the OptiDrill software system. The retraining of the ROP and lithology prediction models based on data from the first wellbore showed promising results, particularly in terms of predictive accuracy and consistency across different drilling parameters. However, it could also be observed that retraining the ROP prediction model on the data from the first wellbore lead to a significantly more optimistic predictive behaviour of the model. This was caused due to the fact that the ROP in general was limited and on average significantly lower during the second field test, than it was during the first round of drilling and accordingly also within the data the model was trained on. Therefore, the MSE and ROP optimisation was also very optimistic regarding the predicted optimised ROP values and the respective calculated MSE values.

While the ROP prediction model did demonstrate improved metrics compared to the first field test, the lithology prediction model encountered challenges, likely due to overfitting and a lack of diverse training data. The results achieved by the drilled lithology model could be improved in the sense that they were more plausible compared to those from the first field test, however the total predictive performance still remained unsatisfactory. One major finding in this regard is that although drilling data, even though it might be derived from drilling projects with very similar equipment and from very similar locations, can still differ quite significantly leading to challenges in creating accurate outputs with specialized machine learning models. Many factors play an import role in this regard, such as local geological properties, changes in the equipment used, or other additional limitation in the drilling strategy. The data from the Geostar 2 project for example, which was used for the model training for the first field test, was derived from a very similar location close to the Push-It drill site. However, a smaller bit diameter used and different local geological settings, posed a significant challenge for the lithology prediction model. The same accounted to the hardware differences between the first and the second wellbore of the Push-It project.

One reasonable solution to tackle the issue of changing parameter ranges could be to enable the manual setting of minimum and maximum thresholds for the drilling process parameters used as inputs to the predictive model. This would be rather easy to implement, e.g. directly into the GUI. This way a custom scaler could be generated for the live adjustment of the processing of the incoming drilling data. At least for the ROP prediction the impact could be directly measured by observing and analysing the error made during the ROP prediction.

Concerning the lithology prediction module one solution could be to further simplify the classification of the types of lithologies. However, since this is a very complex topic and the not only the geological settings, but also drilling equipment and operator behaviour play a very crucial role, this task would require significant additional amounts of data and efforts to be made. Under slightly more favourable conditions, as it has been proven in the respective deliverable reports from work package number 8, the approach applied in the current OptiDrill system prototype is valid and can deliver reasonable results. The anomaly detection module flagged up a significant proportion of the analysed data points as anomalous and might need some further refinements to make the classification less sensitive and prone detected normal data points as anomalous. Since not actual drilling problems were encountered during the two rounds of field testing, it is difficult to make a statement about the frameworks capability to detect a real drilling problem during the drilling operation.

All in all, the second round of field testing the OptiDrill system did provide some additional valuable insights into the systems performance. Unfortunately, due to the changes in equipment between the first and the second wellbore, again the new drilling data did not fit to the data the supervised learning based predictive models were trained on. This shows one major limitation of the system in its current state. Nevertheless, just as during the first field test it could be proven that the system runs without any issues in a real drilling environment and has huge potential to increase the overall performance and process awareness during a drilling operation.

REFERENCES